Rev. Roum. Sci. Techn.– Électrotechn. et Énerg.
Vol.. **67**, *3*, pp. 327–330, Bucarest, 2022

RADIATION OF A SLOT IN HIGH-SPEED DIGITAL SYSTEMS

MIRCEA NICOLAESCU[1], VICTOR CROITORU[2], LEONTIN TUȚĂ[3]

Keywords: Radiation; Slot; Electromagnetic compatibility; High-speed digital systems.

The miniaturization of the digital electronic systems, the increase of the frequency, and the decrease of the power level make the electromagnetic compatibility issues a very important domain in the designing process of digital electronics. Both printed circuit boards (PCBs) and the enclosure of the digital systems contain slots of different dimensions for connectors and expansion cards. If they are excited by currents (common currents) or field distributions, they will radiate electromagnetic energy in the surroundings producing electromagnetic interferences. The paper studies the electromagnetic field radiated by a slot cut in a conductive surface in the frequency range of 1 to 40 GHz.

1. **INTRODUCTION**

In most cases, the digital systems are laid on printed circuit boards (PCBs) with one or more layers. The material used for PCB fabrication depends on several parameters. Among these, from the electrical point of view, the behavior of the dielectric material at the working frequency is a very important parameter. As the applications of digital systems go up in the frequency domain to provide higher data transfer, the dielectric losses in PCB are becoming more important [1]. In high complexity PCB with several layers, one or more ground/reference planes can be used. These ground planes cover the entire surface of the PCB or just specific parts of it, such as the inductance for the return currents to be as low as possible. The conductive surfaces (ground/reference planes or shielding planes, or box walls) can have slots of different dimensions for connectors, cable passing, *etc*. [2]. The currents flowing on these surfaces will generate different distributions of electromagnetic fields on that surfaces that will turn them into electromagnetic interference sources [3].

These kinds of slots can be found on both the front and the rear panel of a desktop, for a universal serial bus (USB), for a digital video disc (DVD), as extensions, a power outlet, an Internet plug, *etc*. [4]. To study the frequency behavior of this radiant structure and its influence on electromagnetic compatibility, the electromagnetic field radiated by a slot corresponding to an extension card is determined by calculus and by simulation.

2. **CALCULUS OF SLOT RADIATION**

To compute the electromagnetic field radiated by a slot cut in a conductive surface, an infinite conductive surface is considered in the *x*O*y* plane. The slot is cut as in Fig. 1 in the middle of the surface. It is supposed that the radiant surface has a certain distribution of the electromagnetic field, with electric field varying along the O*x* axis and magnetic field varying along the O*y* axis, such as the direction of the Poynting vector to be along O*z* axis. This configuration of the electromagnetic field does not limit the generality of the problem, as any distribution of the electromagnetic field can be decomposed into two distributions in two perpendicular planes. Having this distribution of the electromagnetic field, the radiated field in a point P in space, at the distance r0 toward the origin of the coordination system, can be computed. The projection of the point P in the *x*O*y* plane is P'. The radiant surface is split in many elementary surfaces of the dimensions $dx_\Sigma dy_\Sigma$. If the propagation medium is linear and isotropic, then the radiated field in point P can be determined using the superposition theorem, by summing the contributions of all elements $dx_\Sigma dy_\Sigma$ on the surface Σ. If the elementary area is small enough, that the sum turns into an integral [5].

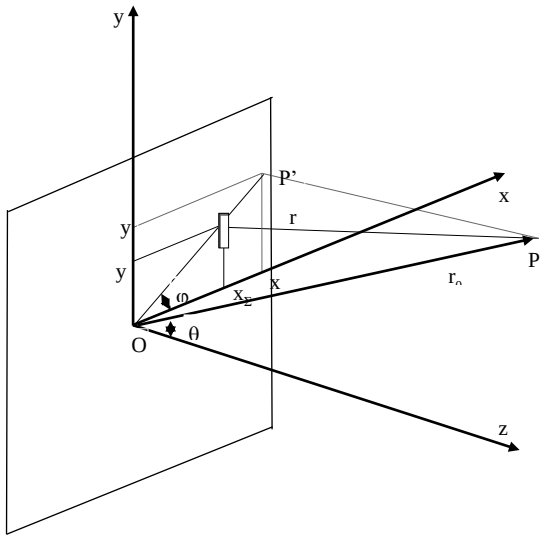

Fig. 1 – The slot geometry for the radiated electric field calculus.

The radiation properties of the elementary area are determined using the electromagnetic field radiated by an infinitesimal conductor fed with a sinusoidal current. The distribution of the electromagnetic field is replaced by distributions of currents, based on the equivalence principle [6]. Then the elementary area is alternatively considered an elementary electric dipole and elementary magnetic dipole [5].

$$E = \mathrm{j}\iint_{\Sigma} \frac{f_1(\varphi,\theta) + f_2(\varphi,\theta)}{2\cdot\lambda} \frac{\mathrm{e}^{-\mathrm{j}\cdot\beta\cdot r}}{r} \cdot E_{x\Sigma}\, \mathrm{d}x_\Sigma\, \mathrm{d}y_\Sigma\ , \qquad (1)$$

where: $f_1(\varphi,\theta)$, $f_2(\varphi,\theta)$ expresses the dependency of the radiated field on φ and θ in a plane that includes the dipole axis and in a plane perpendicular to the dipole axis. Looking at Fig. 1, the distance *r* from a point on surface Σ to point P can be written as:

[1,2] Department of Telecommunications, "Politehnica" University of Bucharest, mircea.nicolaescu@outlook.com, croitoru@adcomm.pub.ro
[3] Department of Communications and Information Technology, Military Technical Academy "Ferdinand I", leontin.tuta@mta.ro

$$r = \sqrt{(x-x_\Sigma)^2+(y-y_\Sigma)^2+z^2} = r_0\sqrt{1-\frac{2xx_\Sigma}{r_0^2}-\frac{2yy_\Sigma}{r_0^2}+\frac{x_\Sigma^2+y_\Sigma^2}{r_0^2}} \cong r_0\left(1-\frac{xx_\Sigma}{r_0^2}-\frac{yy_\Sigma}{r_0^2}\right) = r_0 - x_\Sigma\cdot\sin\theta\cdot\cos\varphi - y_\Sigma\cdot\sin\theta\cdot\sin\varphi \ . \quad (2)$$

Replacing (2) in (1) results:

$$E = \mathrm{j}\cdot\frac{f_1(\varphi,\theta)+f_2(\varphi,\theta)}{2\lambda}\cdot\frac{\mathrm{e}^{-\mathrm{j}\beta r_0}}{r}\cdot \cdot\iint_\Sigma \mathrm{e}^{\mathrm{j}\beta(x_\Sigma\sin\theta\cdot\cos\varphi+y_\Sigma\sin\theta\cdot\sin\varphi)}\cdot E_{x\Sigma}\cdot dx_\Sigma\cdot dy_\Sigma \ . \quad (3)$$

In the case of a rectangular surface ($L_{fx} \times L_{fy}$) having the distribution of $E_{x\Sigma}$ as:

$$E_{x\Sigma} = E_0\cdot\cos\left(\frac{\pi\cdot y_\Sigma}{L_{fy}}\right). \quad (4)$$

For H plane: $\varphi = \pi/2$, $f_1(\varphi,\theta)=1$ and $f_2(\varphi,\theta)=\cos\theta$. The radiated electric field is:

$$E_H = \mathrm{j}\cdot\frac{1+\cos\theta}{2\lambda}\cdot\frac{\mathrm{e}^{-j\beta r_0}}{r}\cdot\iint_\Sigma \mathrm{e}^{\mathrm{j}\beta y_\Sigma\sin\theta}E_{x\Sigma}dx_\Sigma dy_\Sigma \ , \quad (5)$$

$$E_H = \mathrm{j}\cdot\frac{1+\cos\theta}{2\lambda}\cdot\frac{\mathrm{e}^{-\mathrm{j}\beta r_0}}{r}\cdot \cdot\int_{-\frac{L_{fx}}{2}}^{\frac{L_{fx}}{2}} dx_\Sigma\int_{-\frac{L_y}{2}}^{\frac{L_{fy}}{2}} E_0\mathrm{e}^{\mathrm{j}\beta y_\Sigma\sin\theta}\cos(\frac{\pi y_\Sigma}{L_{fy}})dy_\Sigma \ , \quad (6)$$

$$E_H = \mathrm{j}\cdot\frac{1+\cos\theta}{2\lambda}\cdot\frac{\mathrm{e}^{-\mathrm{j}\beta r_0}}{r}\cdot \cdot\int_{-\frac{L_{fx}}{2}}^{\frac{L_{fx}}{2}} dx_\Sigma\int_{-\frac{L_{fy}}{2}}^{\frac{L_{fy}}{2}} \mathrm{e}^{\mathrm{j}\beta y_\Sigma\sin\theta}E_0\cos(\frac{\pi y_\Sigma}{L_{fy}})dy_\Sigma \ , \quad (7)$$

$$E_H = \mathrm{j}\cdot\frac{1+\cos\theta}{2\lambda}\cdot\frac{\mathrm{e}^{-\mathrm{j}\beta r_0}}{r}\cdot L_{fx}L_{fy}E_0\frac{\cos(\pi\frac{L_{fy}}{\lambda}\sin\theta)}{1-\left(\frac{2L_{fy}}{\lambda}\sin\theta\right)^2}. \quad (8)$$

For E plane: $\varphi = 0$, $f_1(\varphi,\theta) = \cos\theta$ and $f_2(\varphi,\theta) = 1$, and the radiated field is:

$$E_E = \mathrm{j}\cdot\frac{1+\cos\theta}{2\lambda}\cdot\frac{\mathrm{e}^{-\mathrm{j}\beta r_0}}{r}\cdot \cdot\iint_\Sigma \mathrm{e}^{\mathrm{j}\beta x_\Sigma\sin\theta}E_{x\Sigma}dx_\Sigma dy_\Sigma \quad (9)$$

$$E_E = \mathrm{j}\cdot\frac{1+\cos\theta}{2\lambda}\cdot\frac{\mathrm{e}^{-j\beta r_0}}{r}\cdot \cdot\int_{-\frac{L_{fx}}{2}}^{\frac{L_{fx}}{2}} \mathrm{e}^{\mathrm{j}\beta x_\Sigma\sin\theta}dx_\Sigma\int_{-\frac{L_{fy}}{2}}^{\frac{L_{fy}}{2}} E_0 dy_\Sigma \ , \quad (10)$$

$$E_E = \mathrm{j}\cdot\frac{1+\cos\theta}{2\lambda}\cdot\frac{\mathrm{e}^{-j\beta r_0}}{r}\cdot E_0 L_{fx}L_{fy}\mathrm{sinc}(\beta\frac{L_{fx}}{2}\sin\theta)\cdot \quad (11)$$

3. SIMULATIONS OF SLOT RADIATION

To study the influence of some slots cut in walls of a desktop enclosure, for different input-output elements, DVD, USB, compact disk read-only memory (CD-ROM), toward the electromagnetic compatibility, the electromagnetic behavior of a radiant surface (slot for an expansion card 20×100 mm) is analyzed [7, 8]. The slot is fed using a lumped port located 7.5 mm from the center of the slot to decrease the input impedance. The distribution of the electric field on the slot is presented in Fig. 2.

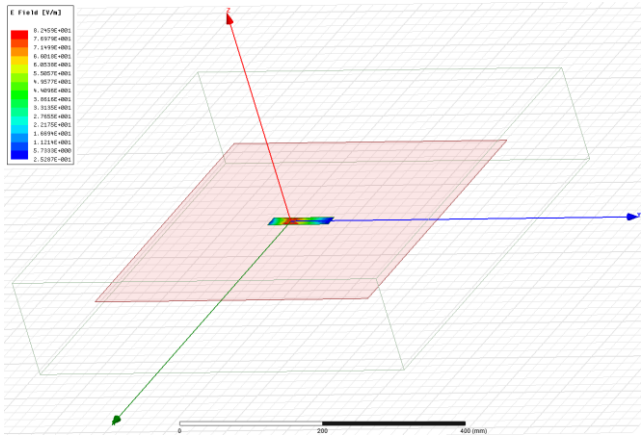

Fig. 2 – The geometry of the radiant structure and the electric field distribution within the slot.

The variation of S_{11} is presented in Fig. 3. The slot is fed with a 50 ohms impedance generator. The input impedance of the slot is still high; this explains the high values of S_{11}. In Fig. 3 one can see that for f = 30.5 GHz S_{11} is –12.8 dB, and for 32 GHz S_{11} is –8 dB. In the frequency range of 5 – 30 GHz S_{11} is in average – 4 dB.

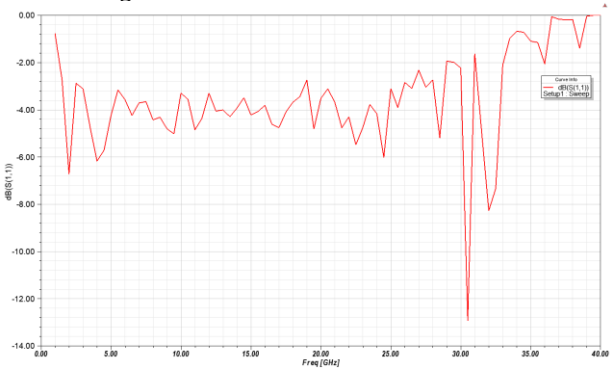

Fig. 3 – The variation of S_{11} of the slot in the frequency range 1 – 40 GHz.

The intensity of the radiated electric field can be derived using *rE* parameter displayed on Fig. 4.

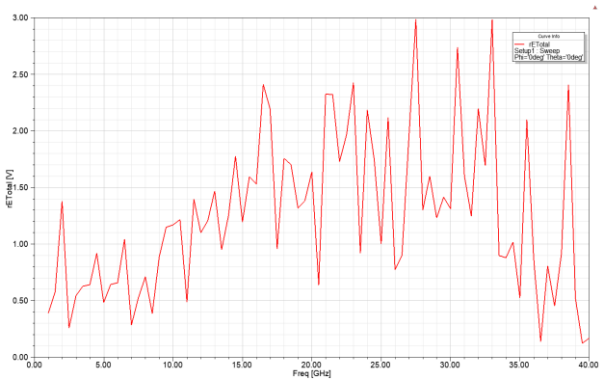

Fig. 4 – The variation of *rE* parameter as a function of frequency for an expansion slot, in the frequency range from 1 to 40 GHz, for $\theta = 0^0$ and $\phi = 0^0$.

The amplitude of the field radiated by the slot depends on the direction, through the angles $\theta = 0^o$ and $\phi = 0^o$, on the frequency, and the distance from the slot to the measuring point. For $\theta = 0^o$ and $\phi = 0^o$, at 1 m, the radiated electric field changes between 0.1 V and 3 V. The highest values are obtained for 27.5 GHz and 34 GHz.

The power applied at the input of the slot through the lumped port is partially reflected and absorbed by the slot. A part of absorbed power is lost in the radiant structure, and most of it is radiated in the medium. The input absorbed and radiated powers as a function of frequency are displayed in Fig. 5. In Fig. 5, in the frequency interval 1 –12.5 GHz, the absorbed and radiated power are almost the same. Theoretically, the radiated power must be lower than the accepted power. Nevertheless, in Fig. 5, some differences can be visualized, and they are caused by the approximation made in the numerical simulations. The maximum difference corresponds to 4 GHz and is 0.004 mW, which means an error of 0.0004 / 0.010 × 100 = 4 %. The radiated power decreases from 8 mW, for $f = 2$ and 4 GHz, to near 0 mW for $f = 40$ GHz. The decrease of the radiated power with the frequency is explained by the fact that the slot operates as a resonant structure. The efficiency diminishes as frequency goes far apart from the resonance frequency.

The radiated field by a slot has components depending on $1/r$, $1/r^2$, and $1/r^3$. The shape of the curve describes the variation of the electric field on the frequency changes from the near field to the far field. At a short distance, 12 cm, the radiated field has local maxima at 20.5 GHz – 34 V/m, 28.5 GHz – 53 V/m, 29.5 GHz – 47 V/m, 35.5 GHz – 46 V/m, and at 38.5 GHz – 30 V/m.

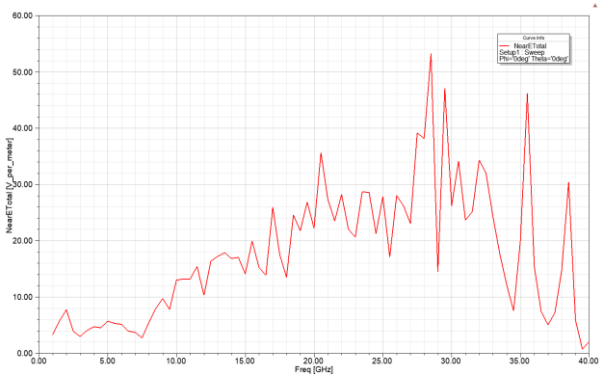

Fig. 6 – The maximum electric field radiated at 120 mm, in the frequency range from 1 to 40 GHz.

The radiated field for 1 – 20 GHz is presented in Fig. 7. It changes from 0.01 V/m to 2.22 V/m, and for low frequencies, 1 – 8 GHz, there is a weak dependency on the angle θ. When frequency increases, the amplitude of the electric field grows in two directions laid symmetrically toward Oz at around 30 and 150º.

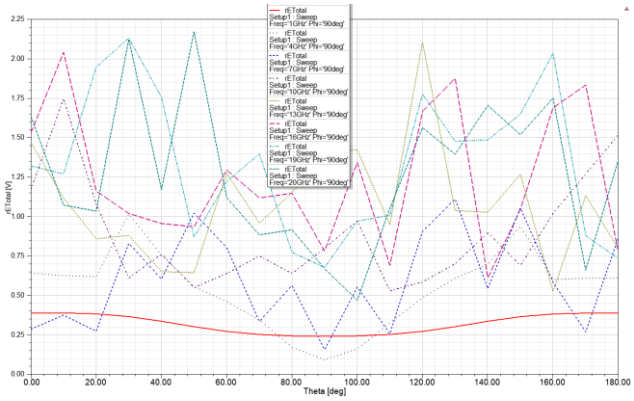

Fig. 7 – The variation of *rE* parameter as a function of angle θ for $f = 1$, 4, 7, 13, 16, 19, 20 GHz and $\phi = 90^0$ for an expansion slot.

The variation of *rE* parameter for $\phi = 0^o$ is displayed in Fig. 8. The maximum value of 2.85 V/m is reached for $\theta = 20^o$.

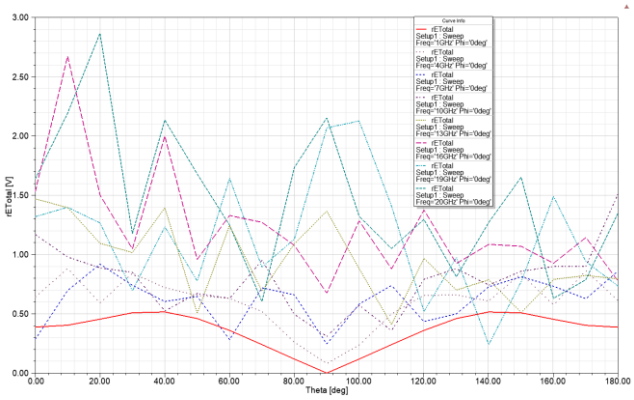

Fig. 8 – The variation of rE parameter as a function of angle θ for $f = 1$, 4, 7, 13, 16, 19, 20 GHz and $\phi = 0^0$ for an expansion slot.

In the frequency band 20 – 40 GHz, as can be seen in Fig. 9, the maximum intensity of the electric field is 2.8 V/m and is obtained for 32 GHz. At higher frequencies, 35, 38, and 40 GHz, the variation of the electric field with angle θ is weaker.

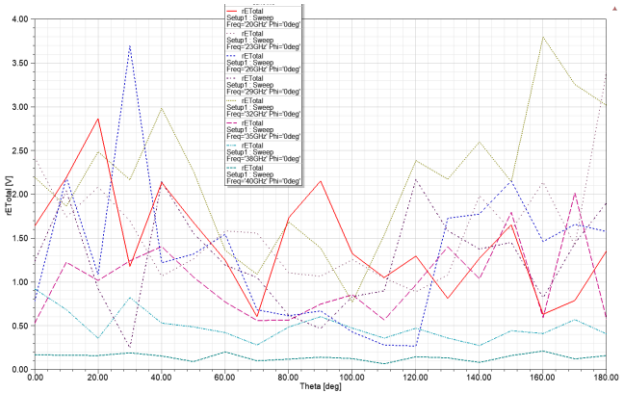

Fig. 9 – The variation of *rE* parameter as a function of angle θ for $f = 20$, 23, 26, 29, 32, 35, 38, 40 GHz and $\phi = 0^0$ for an expansion slot.

Changing the representation plan with 90º ($\phi = 90^o$) the curves from Fig. 10 are obtained. The maximum value of the radiated field is 4 V/m and corresponds to 32 GHz.

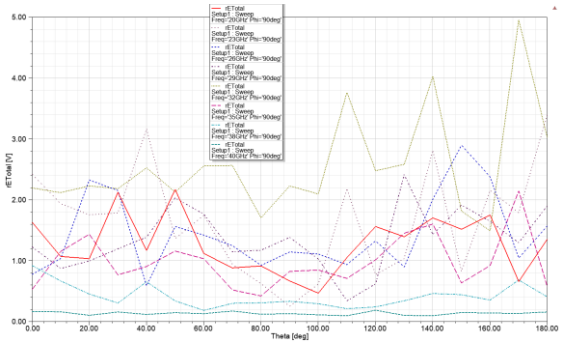

Fig. 10 – The variation of rE parameter as a function of angle θ for f = 20, 23, 26, 29, 32, 35, 38, 40 GHz and $\phi = 90^0$ for an expansion slot.

In the field of electromagnetic compatibility, it is important to know the maximum level of the interference signals generated by an expansion slot. In Fig. 11, the maximum electric field measured on a 1 m ray sphere is presented. The amplitude of the electric field increases linearly from 0.5 V/m to around 1.6 V/m in the frequency range of 1 – 2 GHz. The maximum level of the radiated electric field varies around 1.4 V/m when the frequency changes from 2 GHz to 6.5 GHz. In the frequency band 6.5 GHz and 22.5 GHz, the field grows from 1.4 V/m to 7 V/m, followed by a decrease with 5 local maxima from 22.5 GHz to 40 GHz. The local maxima are obtained at 28.5 GHz (8.5 V/m), 30.5 GHz (9 V/m), 32 GHz (8 V/m), f = 36 GHz (4.8 V/m), and 38.5 GHz (5.4 V/m).

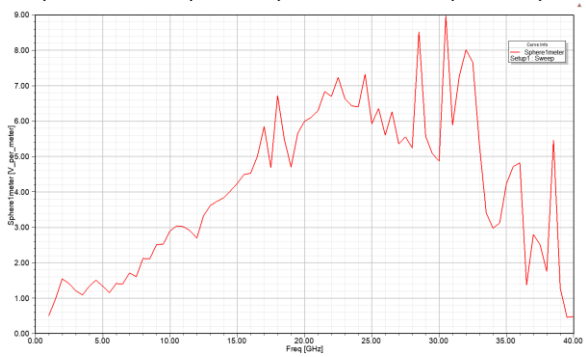

Fig. 11 – The maximum electric field radiated at 1m, in the frequency range from 1 to 40 GHz.

4. **CONCLUSIONS**

High-speed digital systems reach frequencies of the order of GHz, even tens of GHz, which means that the relevant spectral components can be as high as 40 GHz. The paper analyzes the electromagnetic radiation of a slot cut in a reference plane or in a wall of a digital system enclosure. In the first part, the electric field radiated by a slot is determined by calculus, while in the second part, the radiated field is determined by simulations. The variation of the maximum electric field in the frequency band 1 – 40 GHz in the near field and far field, at a certain distance, are presented. Also, the dependencies of the radiated field of frequency and angular coordinates are displayed.

Received on 28 March 2022

REFERENCES

1. I. Plotog, G. Vărzaru, C. Turcu, T. Cucu, P. Svasta, N. Codreanu, *EMC requirements for DFM multicriterial approach*, Rev. Roum. Sci. Techn. – Électrotechn. et Énerg., **53** (Suppl.), pp. 155–165 (2008).
2. H.B. Bakoglu, *Circuits, Interconnections, and Packaging for VLSI*, Addison Wesley, Upper Saddle River, NJ, 1990.
3. Y. Fu, T. Hubing, *Analysis of radiated emissions from a printed circuit board using expert system algorithms*, IEEE Transactions on Electromagnetic Compatibility, **49**, *1*, pp. 68-75 (2007).
4. G. Cerri, R.De Leo, V.M. Primiani, *Theoretical and experimental evaluation of the electromagnetic radiation from apertures in shielded enclosures*, IEEE Transactions on Electromagnetic Compatibility, **34**, *4*, pp. 432-433 (1992).
5. L. Buzinu, L. Anton, D. Deparateanu, M. Nicolaescu, *Analysis of an array of rectangular apertures based on the active parameters of its infinite extension*, 12th Intern. Conf. on Comm., Bucharest, 2018.
6. J. D. Kraus, *Antennas and Wave Propagation*, Mc Graw-Hill, Inc, U.S.A., 2017.
7. C. Poschalkoand S. Selberherr, *Calculation of the radiation from the slot of a slim enclosure with a cavity resonator model*, Asia-Pacific Symposium on Electromagnetic Compatibility and 19th Int. Zurich Symposium on Electromagnetic Compatibility.
8. M. Li, J. Nuebel, J.L. Drewniak, R.E. DuBroff, T.H. Hubing, T.P. Van Doren, *EMI from cavity modes of shielding enclosures – FDTD modeling and measurements*, IEEE Transactions on Electromagnetic Compatibility, **42**, *1*, pp. 29–38 (2000).